SAR SIMULATION FOR CHIRAL WAVES IN HEAD MODEL

Héctor Torres S.[1] **Mario Zamorano L.**[1]

Received july 22, 2003, accepted august 25, 2003

ABSTRACT

A numerical model of an electromagnetic wave, propagating in a chiral media, characterized by the Born-Fedorov formalism, is presented. FDTD numerical method, adapted to chiral media, is used. The classical Yee algorithm, implemented by several authors for non chiral media, does not provide, for the same time instant, knowledge of the transverse field components (both incident and induced by the chirality). This problem is solved by the authors, delaying one of the field components when it incides in the achiral-chiral interface, storing the values corresponding to the times n and n –1, in order to solve for the the field at time n+1. The simulation results of propagating Gaussian pulses in chiral media, in the range of microwaves, show the chiral curl of the polarization plane. The results show that the use of the box model in combination with a realistic model of the head derived of a resonance image, is important for accurate determination of the near chiral fields induced in the head. It was found that, through SAR (Specific Absorption Rate) parameter, about 20% of the antenna input power is absorbed in the head. It is proposed that the chiral effect is due to a microscopic mechanism, where the typical cell membrane is a fairly fluid bilipid layer, with a few big protein molecules embedded in it. Every protein molecule is polar and will tend to align itself with an electric field and often rotate helically in its socket, so any volume of brain tissue must have a few cells bearing protein molecules that happen to resonate at its rotation frequency.

Keywords: Maxwell equations, chirality, FDTD, SAR

INTRODUCTION

In this work it is assumed that the brain tissue media is chiral. This chiral effect is due to a microscopic mechanism where the typical cell membrane is a fairly fluid bilipid layer with a few big protein molecules embedded in it. Every protein molecule is polar and will tend to align itself with an electric field and often helical rotate it in its socket, so any volume of brain tissue must have a few cells bearing protein molecules that happen to resonate at its rotation frequency. In the Appendix it presents the basis of the model that it usage for to characterize the microwave absorption waves by the brain tissue when is radiated by the cellular phones.

In relation to helical molecules, a single electrodynamic model is assumed, which allows us to find the averaged electric current knowing the polarization and magnetization [1]. For typical double helices, giving the moment of inertia per unit length, appears a torsional factor. For a given length of a typical chain, we can find that for proteins with a rotation of 90°, corresponds to 1 ev/A°, torsion constant of 0.4 ev/A°, moment of inertia = 100 auA° and the length is 475A°. Here we find that the frequency falls in the interval between 1 GHz and 10 GHz. These frequencies are typical for microwave radiation. In our electrodynamic approach, the connection between these mechanical parameters with the chirality and dielectric properties of the brain tissue considered as a bioplasma is made. In this paper, it consider the Born-Fedorov constitutive equations

$$\boldsymbol{D} = \boldsymbol{e}\left(\boldsymbol{E} + \boldsymbol{b}\nabla\times\boldsymbol{E}\right) \qquad (1.a)$$

$$\boldsymbol{B} = \boldsymbol{m}\left(\boldsymbol{H} + \boldsymbol{b}\nabla\times\boldsymbol{H}\right) \qquad (1.b)$$

where $\boldsymbol{e}$, $\boldsymbol{m}$ and $\boldsymbol{b}$ are the permittivity, permeabilitty and chiral pseudoscalar respectively. Here, the rotor of polarization plane can be predicted from Maxwell equations, considering that the $\boldsymbol{P}$ $\boldsymbol{(M)}$ vector has a proportional additional term to $\nabla\times\boldsymbol{E}$ $(\nabla\times\boldsymbol{H})$ [1], [4].

In linear, isotropic, non-dispersive and chiral materials we can relate D and B. If it is assumed that the medium is isotropic, non-permeable and non dispersive, the Cartesian field components are [2], [7].

[1] , mzamorano@utacl.htorres@uta.clUniversidad de Tarapacá, Departamento de Electrónica, Casilla 6-D, Arica - Chile,

$$D_x = e_0 e_r E_x + e_0 e_r b \left[\frac{\partial E_z}{\partial y} - \frac{\partial E_y}{\partial z} \right] \quad (2.a)$$

$$D_y = e_0 e_r E_y + e_0 e_r b \left[\frac{\partial E_x}{\partial z} - \frac{\partial E_z}{\partial x} \right] \quad (2.b)$$

$$D_z = e_0 e_r E_z + e_0 e_r b \left[\frac{\partial E_y}{\partial x} - \frac{\partial E_x}{\partial y} \right] \quad (2.c)$$

$$B_x = m_0 H_x + m_0 b \left[\frac{\partial H_z}{\partial y} - \frac{\partial H_y}{\partial z} \right] \quad (3.a)$$

$$B_y = m_0 H_y + m_0 b \left[\frac{\partial H_x}{\partial z} - \frac{\partial H_z}{\partial x} \right] \quad (3.b)$$

$$B_z = m_0 H_z + m_0 b \left[\frac{\partial H_y}{\partial x} - \frac{\partial H_x}{\partial y} \right] \quad (3.c)$$

Using the MKS system of units, the following system of scalar equations is equivalent to Maxwell's equations in the rectangular coordinate system (x, y, z).

$$\frac{\partial H_x}{\partial t} = -\frac{1}{m} \frac{\partial E_z}{\partial y} + bw k_y H_z \quad (4.a)$$

$$\frac{\partial H_y}{\partial t} = \frac{1}{m} \frac{\partial E_z}{\partial x} - bw k_x H_z \quad (4.b)$$

$$\frac{\partial H_z}{\partial t} = \frac{1}{m} \left(\frac{\partial E_x}{\partial y} - \frac{\partial E_y}{\partial x} \right) + bw \left(k_x H_y - k_y H_x \right) \quad (4.c)$$

$$\frac{\partial E_x}{\partial t} = \frac{1}{e} \frac{\partial H_z}{\partial y} + bw k_y E_z - s E_x \quad (5.a)$$

$$\frac{\partial E_y}{\partial t} = -\frac{1}{e} \frac{\partial H_z}{\partial x} - bw k_x E_z - s E_y \quad (5.b)$$

$$\frac{\partial E_z}{\partial t} = \frac{1}{e} \left(\frac{\partial H_y}{\partial x} - \frac{\partial H_x}{\partial y} \right) + bw \left(k_x E_y - k_y E_x \right) - s E_z \quad (5.c)$$

Where $w = 2p f$, $k_x = 2p / l_x$ y $k_y = 2p / l_y$.

In the above system of differential equations we see that the vectorial components of the electric flux are related with the respective electric field components and furthermore are proportional to the partial derivative of their orthogonal components.

The main difficulty for an analytic treatment of this system is in the partial derivatives of space and time in which the chiral parameter is present. For this reason, equations (4) and (5) can't be reduced to a typical differential equation with known solution.

DISCRETIZATION BY FDTD

The FDTD method (Finite Difference Time Domain) initially proposed by Yee is commonly used in the resolution of Maxwell equations. It has the advantages that it is not necessary to derive the wave equation of the system in order to solve the field vectors and it operates in the time domain which allows analysis of transient phenomenon. Through the FDTD method, the dicretization of above equations is performed. Before that, it's important to consider the partial derivative approximations made by Mur for achiral-chiral interface case [3], [5].

$$\left. \frac{\partial^2 U}{\partial x \partial t} \right|_i^n = \frac{1}{2\Delta t} \left(\left. \frac{\partial U}{\partial x} \right|_i^{n+1} - \left. \frac{\partial U}{\partial x} \right|_i^{n-1} \right) = \frac{1}{2\Delta t} \left[\left(\frac{U|_{i+1/2}^{n+1} - U|_{i-1/2}^{n+1}}{\Delta x} \right) - \left(\frac{U|_{i+1/2}^{n-1} - U|_{i-1/2}^{n-1}}{\Delta x} \right) \right] \quad (6)$$

Using the Yee basic algorithm notation, the equations are transformed to

$$H_x\big|_{i-1/2,j+1}^{n+1} = H_x\big|_{i-1/2,j+1}^{n} - C_{ay}\left(E_z\big|_{i-1/2,j+3/2}^{n+1/2} - E_z\big|_{i-1/2,j+1/2}^{n+1/2}\right) + C_{qy}\,H_z\big|_{i-1/2,j+1}^{n} \quad (7.a)$$

$$H_y\big|_{i,j+1/2}^{n+1} = H_y\big|_{i,j+1/2}^{n} + C_{ax}\left(E_z\big|_{i+1/2,j+1/2}^{n+1/2} - E_z\big|_{i-1/2,j+1/2}^{n+1/2}\right) - C_{qx}\,H_z\big|_{i,j+1/2}^{n} \quad (7.b)$$

$$H_z\big|_{i,j+1}^{n+1} = H_z\big|_{i,j+1}^{n} + C_{ay}\left(E_x\big|_{i,j+3/2}^{n+1/2} - E_x\big|_{i,j+1/2}^{n+1/2}\right) - C_{ax}\left(E_y\big|_{i+1/2,j+1}^{n+1/2} - E_y\big|_{i-1/2,j+1}^{n+1/2}\right) + C_{qx}\,H_y\big|_{i,j+1}^{n+1/2} - C_{qy}\,H_x\big|_{i,j+1}^{n+1/2} \quad (7.c)$$

$$E_x\big|_{i,j+1/2}^{n+1/2} = D_a\big|_{i,j+1/2}\,E_x\big|_{i,j+1/2}^{n-1/2} - D_{by}\Big|_{i,j+1/2}\left(H_z\big|_{i,j+1}^{n} - H_z\big|_{i,j}^{n}\right) + D_{qy}\,E_z\big|_{i,j+1/2}^{n-1/2} \quad (8.a)$$

$$E_y\big|_{i-1/2,j+1}^{n+1/2} = D_a\big|_{i-1/2,j+1}\,E_y\big|_{i-1/2,j+1}^{n-1/2} - D_{bx}\big|_{i-1/2,j+1}\left(H_z\big|_{i,j+1}^{n} - H_z\big|_{i-1,j+1}^{n}\right) + D_{qx}\big|_{i-1/2,j+1}\,E_z\big|_{i-1/2,j+1}^{n-1/2} \quad (8.b)$$

$$E_z\big|_{i-1/2,j+1/2}^{n+1/2} = D_a\big|_{i-1/2,j+1/2}\,E_z\big|_{i-1/2,j+1/2}^{n+1/2} + D_{bx}\big|_{i-1/2,j+1/2}\left(H_y\big|_{i,j+1/2}^{n} - H_y\big|_{i-1,j+1/2}^{n}\right) - D_{ay}\big|_{i-1/2,j+1/2}\left(H_x\big|_{i+1/2,j+1}^{n} - H_x\big|_{i+1/2,j}^{n}\right) + D_{qx}\,E_y\big|_{i-1/2,j+1/2}^{n-1/2} - D_{qy}\,E_x\big|_{i-1/2,j+1/2}^{n-1/2} \quad (8.c)$$

Where:

$$C_{ay} = \frac{\Delta t}{m_0 \Delta y},\ C_{ax} = \frac{\Delta t}{m_0 \Delta x}$$

$$C_{qy} = bw k_y \Delta t,\ C_{qx} = bw k_x \Delta t$$

$$D_a\big|_{i,j} = \frac{2e_{i,j} - s_{i,j}\Delta t}{2e_{i,j} + s_{i,j}\Delta t}$$

$$D_{by}\big|_{i,j} = \frac{2\Delta t/\Delta y}{2e_{i,j} + s_{i,j}},\ D_{bx}\big|_{i,j} = \frac{2\Delta t/\Delta x}{2e_{i,j} + s_{i,j}}$$

$$D_{qy} = \left(bw k_y \Delta t\right) \Big/ \left(1 + \frac{s_{i,j}\Delta t}{2e_{i,j}}\right)$$

$$D_{qx} = \left(bw k_x \Delta t\right) \Big/ \left(1 + \frac{s_{i,j}\Delta t}{2e_{i,j}}\right)$$

Here, it is assumed that a grid point in space is defined as (i, j, k) with coordinates (iΔx, jΔy, kΔz) where Δx=Δy=Δz=Δ is the cubic cell size and Δt is the time increment.

An important problem encountered in solving the time domain electromagnetic-field equation, by FDTD method is the absorbing boundary conditions. In our formulation, the second order approximation of Mur is used for the near-field irradiation problems. The external absorbing are placed at a distance of 4-7Δ on all sides of the human head model. In our near-field simulation we have 64,000 cubic cells of 5 mm side each. The radiation source of the cellular phone was modeled by an equivalent dipole antenna. After having obtained the induced chiral electric field by the FDTD method, the local specific absorption rate SAR, is calculated as [5]:

$$SAR_{i,j} = \frac{\sigma_{i,j}\,E_T^2\big|_{i,j}}{2\rho_{i,j}} \quad (9)$$

where $$E_T\big|_{i,j} = \sqrt{\frac{1}{n}\sum_{1}^{n} E_y^2\big|_{i,j}^{n} + E_x^2\big|_{i,j}^{n} + E_z^2\big|_{i,j}^{n}}$$

In these equations, the electric (magnetic) fields depend not only on E (resp. H) but also on the transverse components. In effect, there is coupling between the eq. (8.a) and (8.b) through terms $E_z\big|_i^{n+1}$ and $E_y\big|_i^{n+1}$. In this way, a new difficulty appears: the impossibility of knowing both variables at the same time. This is solved delaying one of the fields when it incides in the achiral-chiral interface, then the fields at the steps n and $n-1$ are stored for the evaluation of the respective $(n+1)$ field [6].

NUMERICAL RESULTS

Using the linear FDTD algorithm with chirality, obtained from equations (7) and (8), some simulations for the microwave spectrum are made. These simulations start with a *y*-polarized Gaussian pulse, generated in the free space and propagating in the *x* direction to the achiral-chiral interface [7], [8].

Simulation 1: A 1 [*V/m*] of amplitude Gaussian pulse with his bandwidth 1.8 GHz. The spatial grid is Δx = 2.94 [*mm*] with time step of 7.353 [*ps*], and Courant factor S = 0.75, value that secures the system stability. The media has a chiral factor $\beta = -0.15\times10^{-3}$ [*m*], a relative permittivity equal to 40 and is placed at $70\Delta x$ from the domain boundary. After 150 time steps of simulation, the following results are obtained:

The Figs. 1 and 2 show, after 150 time steps, the polarized pulse in *y* direction and its rotation to the *z* transversal axis, that is to say, there is a component E_z in the chiral media, which is a brain tissue model. These results are a consequence of curl equations (2) and (3). In the Fig. 1 the transversal angle, formed between E_y and E_z is 8.24º, and the module is $|E_{max}| = 0.472$ [*V/m*]. Besides, the pulse looses part of its initial energy due to the reflexion in the interface, because of the high medium permittivity.

Simulation 2: Gaussian pulse with 1 [*V/m*] of amplitude has a bandwidth 0.9 GHz. The spatial grid is Δx = 2.5466 [*mm*] with time step of 6.371 [*ps*], and Courant factor S = 0.75. The media has a chiral factor $\beta = -0.15\times10^{-3}$ [*m*], a relative permittivity equal to 40 and is placed at $70\Delta x$. After 150 time steps of simulation the following results are obtained:

The Fig. 2 shows the electric field module, 0.4521 [*V/m*] and the transversal angle is 12.7º, which signify that there is higher rotation of vectors *E* and *H*. It´s observed a reduction of the resultant pulse amplitude in comparison with the simulation 1; it is due to the dielectric permittivity, but the chiral effect is more strong.

Simulation 3: The human head model was constructed with 64,000 cubic cells. The total numbers of layers used in this model was 50. The 35 th layer counted from the bottom of the head , with each cell size of 0.5 cm is shown in Fig. 3. Both the dielectric constant and the conductivity of the brain were obtained from literature [5], [6]. The calculations were made with an initial sinusoidal time varying electric field. The chiral factor was $\beta = -0.00015$.

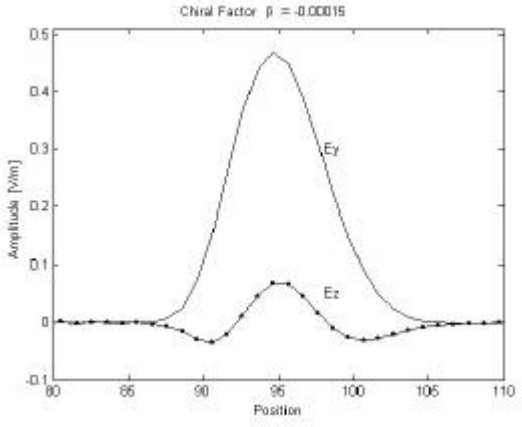

Fig. 1.- Electric field components inside a chiral medium with β = –0.00015 for excitation frequency of 1.8 GHz.

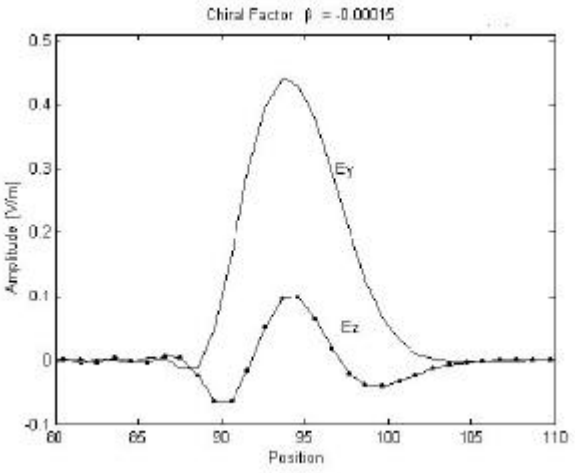

Fig. 2.- Electric field components inside a chiral medium with β = –0.00015 for excitation frequency of 0.9 GHz.

Fig. 3 shows the structure with different layers, considering the brain layer as a chiral media. The factor β takes different values. Figs. 4 and 5 show the simulated SAR for positive and negative β. In the Fig.6 we can see the simulated electric field in the brain layer for different values of the chiral factor. Here the Electric field is enhanced by the factor β. In Figs. 7 and 8 we plot the SAR simulation for a chirohead model Here the absorption of microwave radiation increases when the chiral factor CF= β increases. In the last figure that value 0db corresponds to the input power.

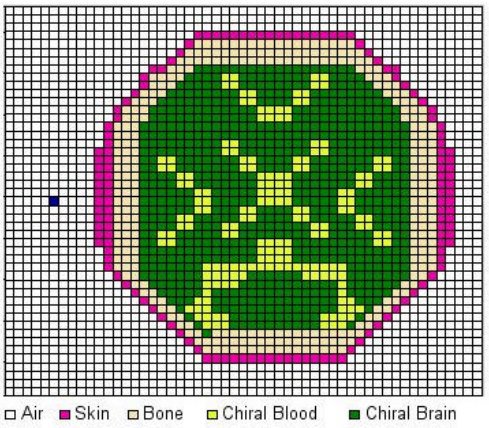

Fig. 3.- The structure at layer 35 counted from the bottom of the human head model

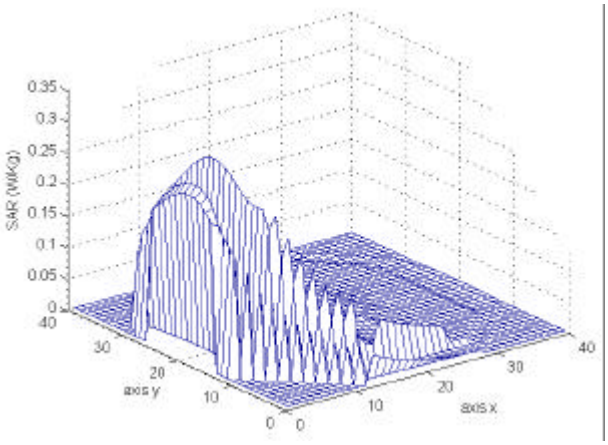

Fig. 4.- SAR simulation in 2-Dimensions for a chiral brain layer $b = -0.5$

Fig. 4 shows the SAR distributions taking into account only the chiral effect. These results can be added to the typical results obtained by other authors [5], [6]. This represents about 20% of the antenna input power which is absorbed in the head.

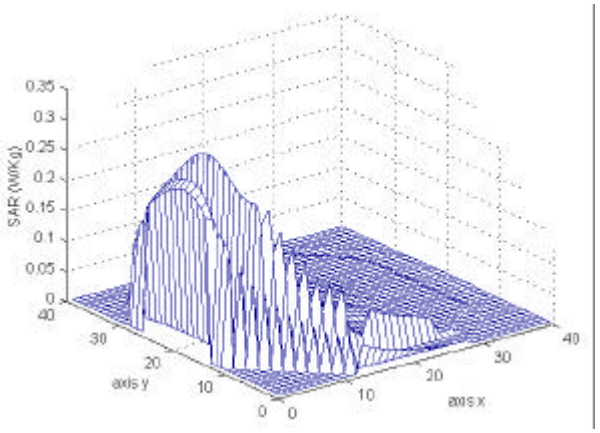

Fig. 5.- SAR simulation in 2-Dimensions for a chiral brain layer $b = 0.5$

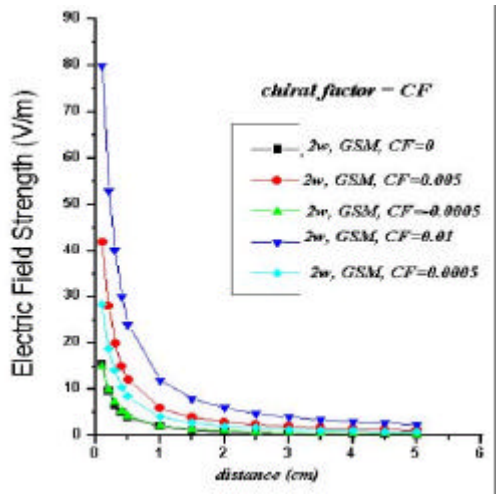

Fig. 6.- Electric field strength versus distance having the chiral factor CF= b as a parameter, for a cell phone

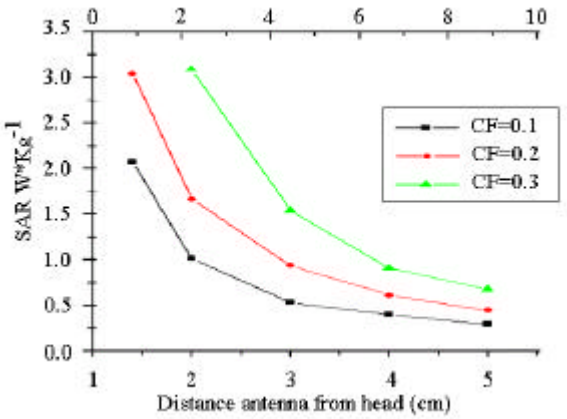

Fig. 7.- SAR vs distance for different values of CF= b . SAR values in W/Kg per Watt of antenna output averaged over 10 gr. of tissue at 900 MHz and show for three values of chiral parameter (Fondecyt 1010300)

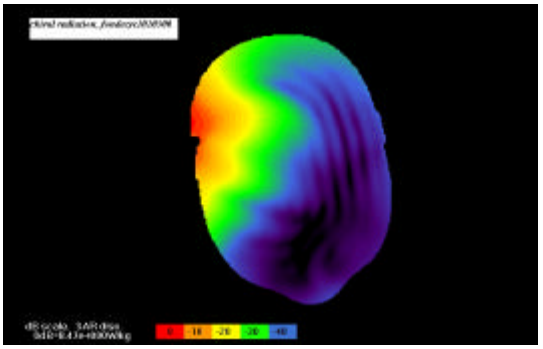

Fig. 8.- SAR simulation in a chirohead model (CF=0.1)

CONCLUSIONS

The Born-Fedorov formalism was used to model the temporal electric and magnetic fields, where the chiral parameter b represents the module and rotation of the fields inside the medium.

In this paper propagation of Gaussian pulses in the chiral materials was modeled. The FDTD method for the numerical calculation was used. Results show the chirality effect on *TEM* input pulse. In the microwave range, the rotation of the electromagnetic field, that is the chirality factor of the brain layer that enhance the SAR factor and the electric field in the brain layer considered as a chiral media, are shown.

ACKNOWLEDGMENTS

The authors thank the Chilean Agency CONICYT for their financial support. FONDECYT No. 1010300, and University of Tarapacá Projects Nºs. 8721-03 and 8722-03. Also we greatly appreciate the help received from M Sc. Enrique Fuentes H.

REFERENCES

[1] H. Torres Silva; "Waves in a Chiral-Plasma Media", The Japanese Journal of Physics, Vol. 67, pp. 850-857, 1998.

[2] Taflove and S.C. Hagness; "Computational Electrodynamics: The Finite-Difference Time Domain Method", Artech House, Second Edition, 2000.

[3] V. Lindell, A. H. Sihvola, S.A Tretyakov and A. J. Viitanen; "Electromagnetic Waves in Chiral and Bi-isotropic Media", Artech House, Second Edition, 2000.

[4] H. Torres Silva; "Propagación de Ondas Pulsadas en un Chiroplasma Magnetizado", Rev. Mexicana de Física, N° 44 Supl. 3, pp. 53.58, Dic. 1998.

[5] K. S. Yee; "Numerical solution of initial boundary value problems involving Maxwell's equations in isotropic media", IEEE Trans. Antennas Propagat, Vol. AP-14, N° 5, pp. 302-307, 1966.

[6] H. Chen, H. Wang; "Current and SAR Induced in Human Head Model by the Electromagnetic Fields Irradiated from a Cellular Phone", IEEE Trans. Microwave Theo. And Tech, Vol. 42, N° 12, pp. 2249-2254, 1994.

[7] F. Ortiz; "Análisis de la Propagación de Ondas Electromagnéticas en Medios Quirales Mediante el método FDTD", Proyecto de Título Ing. Civil Electrónica, UTA, 2001.

[8] H. Torres Silva, M. Zamorano; "FDTD Algorithm Used to Calculate the RF Chiral Waves in the Human Head", 2nd International Workshop Biological Effects of EMFs, Rodees -Grecia, 2002.

APPENDIX

Basis of bioplasmatic-chiral model (*)

The brain skin is a thin layer of neurons inter-connected that overlap the cerebral hemisphere irregular surface. The neurons are protein synthesized cells characterized by:

- Complex shapes and a large surface of cellular membrane.
- Producing different types of products to level of their axonics terminals.
- Requiring a constant re-exchange of their organelles and molecular elements.

The structural characteristics of neurons are given by their basic elements: the some, the dendrites and the axon. The neuronal body is surrounded by a bulk membrane of 7.5 nm approximately, called plasmatic membrane. The cytoplasm is the material comprised between the plasmatic membrane and the nuclear envelope and presents a series of membranous systems that form organelles inter-connect (Fig. 9).

The cellule form is supported by fibroses protein that meeting in the cytoplasm and the conjunct form the cytoskeleton, which is a dynamical tridimensional structure that overflow the cytoplasm and it is transparent therefore invisible. To stabilize the cell structure, to organize the cytoplasm with all organelles and to produce motion is their function. It is formed by different types of filaments, thereamong are the actin filaments and the microtubules. The actin is a protein that associate spontaneously by itself to form a linear and helicoidal polymer. These filaments are important in the cell motion and in the cellular structure. The microtubules are hollow cylinder with protein of 25 nm outer diameter approximately and 14 nm of inner diameter. They are formed by two protein subunits called tubulins (dimmers) a and b, coupled helicoidally in 13 lines and by microtubules associated proteins (MAPs) (Fig. 10).

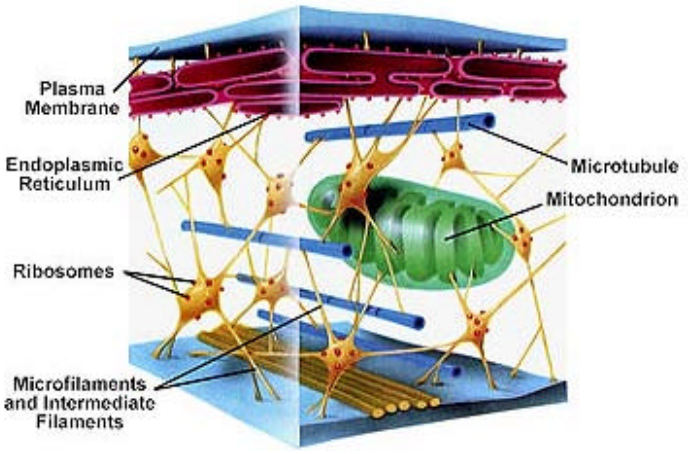

Fig. 9.- Neuron structure

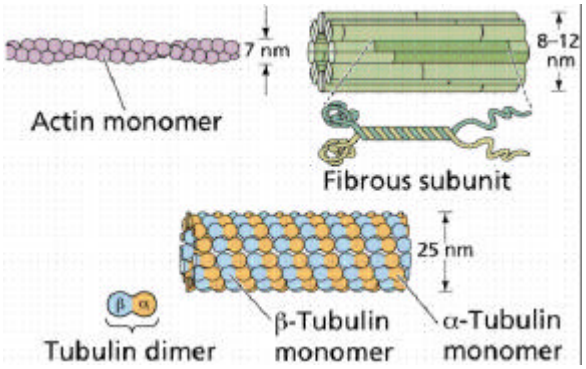

Fig. 10.- Microtubules in tubulin a and b

(*) http://users.rcn.com/jkimball.ma.ultranet/BiologyPages/C/Cytoskeleton.html
http://cellbio.utmb.edu/cellbio/microtubule_structure.htm